HIBISCUS PUBLISHER

JOURNAL OF ENVIRONMENTAL MICROBIOLOGY AND TOXICOLOGY

Website: https://journal.hibiscuspublisher.com/index.php/JEMAT

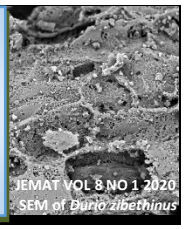


# Mathematical Modelling of the Growth of SARS-CoV-2 (COVID-19) and SARS-CoV (SARS) Viruses in Vero E6 Cells

Mohd Yunus Abd Shukor[1]* and Mohammad Shafiul Alam[2]

[1]Department of Biochemistry, Faculty of Biotechnology and Biomolecular Sciences, Universiti Putra Malaysia, 43400 UPM Serdang, Selangor, Malaysia.
[2]Infectious Diseases Division, International Centre for Diarrhoeal Disease Research, Bangladesh (ICDDR,B), Dhaka-1212, Bangladesh.

*Corresponding author:

Prof. Dr. Mohd Yunus Shukor,
Department of Biochemistry,
Faculty of Biotechnology and Biomolecular Sciences,
Universiti Putra Malaysia,
43400 UPM Serdang, Selangor,
Malaysia.
Email: mohdyunus@upm.edu.my

**HISTORY**

Received: 20th June 2020
Received in revised form: 30th June 2020
Accepted: 1st July 2020

**KEYWORDS**

SARS-CoV-2
SARS-CoV
Vero E6 cells
growth curve
modified Logistics

**ABSTRACT**

COVID-19 is caused by the coronavirus SARS-CoV-2 which shares genetic similarity to the agent for the SARS virus (SARS-CoV). The growth of these two viruses in Vero E6 cells shows sigmoidicity and hence various primary growth models can be applied to extract useful growth parameters. The overlapping of the 95% confidence intervals for the parameters $A$ (lower asymptote value of virus titer) and $\mu_m$ (maximum specific viral titer) in the modified Logistics model indicates no significant differences between these two parameters. However, the $y_{max}$ or viral titer log (PFU/mL) upper asymptote values did not overlap suggesting significant differences between the two values with viral titer values for SARS-CoV (SARS) value higher than SARS-CoV-2 (COVID-19). The result obtained in this study warrants further study to the infection rate for both viruses that can be useful in studying potential similarity and differences between the two viruses.

## INTRODUCTION

The SARS-CoV-2 virus is the agent causing the global pandemic COVID-19 which is still ravaging the human population with the current death tolls exceeding half a million people and more than 10 million people are infected [1]. Worldwide societies and economies have come to a near-complete standstill for the first time in a century because of this virus. The virus belongs to the family of coronavirus (CoV), which is known to have given rise to zoonotic infections over the past centuries on many occasions [2]. To date, seven CoVs segregated into two classes have been identified that can cause infections in humans. There are four endemic human CoVs (HCoVs) in one group, the first of which was reported in the 1960s, causing large numbers of common colds annually [3]. Three zoonotic CoVs form the other group that have recently caused outbreaks and include SARS— the severe acute respiratory syndrome coronavirus in 2002–2003, MERS— the Middle East respiratory syndrome-coronavirus since 2012 and COVID-19—the current SARS-CoV-2 pandemic. SARS-CoV-2 first emerged near the city of Wuhan in the People Republic of China in the fall of 2019 [2,4–6].

The newly emerging SARS-CoV-2 was quickly identified as a coronavirus with relatively close in genomic identity (~80 % identical) to the 2003 SARS-CoV virus. In addition, the organization of Open Reading Frames (ORFs) in the two viruses is highly similar. The International Committee on the Taxonomy of Viruses classifies the new agent to be within the severe acute respiratory syndrome-related coronavirus (including the 2003 SARS-CoV) based on the sequence identity of the amino acids of the viral proteins that was found generally ranges 65% in the least conserved parts of the S protein to approximately 95% in the most conserved replicative enzyme domains [5,7,8].

Both of these viruses are likely to share similar molecular biology based on the close phylogenetic relationship. This means that the accumulated knowledge on SARS can be useful in studying the molecular biology of SARS-CoV-2. Such similarity has been reported, which include a similar angiotensin-converting enzyme 2 (ACE2) receptor entry port for the two viruses [7,9–11]. The ACE2 receptor is copiously expressed in the African green monkey kidney cells (Vero cells), and the cells

have been used extensively in research for studying the cell-culture-based infection models of SARS-CoV [12–14].

In a previous publication, the growth curves of SARS-CoV-2 and SARS-CoV in Vero E6 cells was compared for the first time. Both of the growth curves appears sigmoidal [12] and hence can be model using various standard primary models such as the popular modified Gompertz and modified Logistics [15–18]. The aim of this study is to apply the two models above to the growth curves of the viruses in Vero E6 cells.

## MATERIALS AND METHODS

Data for Figure **1** were digitized using the software Webplotdigitizer 2.5 [19] from a published work [12]. Digitization using this software has been acknowledged for its reliability [20,21]. The data were then nonlinearly regressed using the curve-fitting software CurveExpert Professional software (v.1.6.3, http://www.curveexpert.net/, USA)) using two popular models often used to model microorganism growth—modified logistics **(Equation 1)** and modified Gompertz **(Equation 2)** [15,22].

$$y=\frac{A}{\left\{1+\exp\left[\frac{4\mu_m}{A}(\lambda-t)+2\right]\right\}} \qquad \textbf{(Eqn. 1)}$$

$$y=A\exp\left\{-\exp\left[\frac{\mu_m e}{A}(\lambda-t)+1\right]\right\} \qquad \textbf{(Eqn. 2)}$$

Note:
A= Viral titer log (PFU/mL) lower asymptote;
$\mu_m$= maximum specific viral titer log (PFU/mL) growth rate;
λ=lag time (h.p.i)
$y_{max}$= Viral titer log (PFU/mL) upper asymptote;
e = exponent (2.718281828)
t = sampling time (h.p.i)

### Statistical analysis

Commonly used statistical discriminatory methods such as corrected AICc (Akaike Information Criterion), Root-Mean-Square Error (RMSE), and adjusted coefficient of determination ($R^2$) were utilized to find the best models from the two.

The RMSE was calculated according to **Eqn. 1** [23], and a smaller number of parameters is expected to give a smaller RMSE value. $n$ is the number of experimental data, $Ob_i$ and $Pd_i$ are the experimental and predicted data, while $p$ is the number of parameters.

$$RMSE=\sqrt{\frac{\sum_{i=1}^{n}(Pd_i-Ob_i)^2}{n-p}} \qquad \textbf{(Eqn. 1)}$$

As $R^2$ or the coefficient of determination ignores the number of the parameter in a model, the adjusted $R^2$ is utilized to overcome this issue. In the equation (**Eqns. 2** and **3**), the total variance of the y-variable is denoted by $S^2_y$ while RMS is the Residual Mean Square.

$$Adjusted\left(R^2\right)=1-\frac{RMS}{s_Y^2} \qquad \textbf{(Eqn. 2)}$$

$$Adjusted\left(R^2\right)=1-\frac{\left(1-R^2\right)(n-1)}{(n-p-1)} \qquad \textbf{(Eqn. 3)}$$

The Akaike Information Criterion (AIC) is based on information theory. It balances between the goodness of fit of a particular model and the complexity of a model [24]. To handle data having a high number of parameters or a smaller number of values corrected Akaike information criterion (AICc) is utilized [25]. The AICc is calculated as follows (**Eqn. 4**), where $p$ signifies the quantity of parameters and $n$ signify the quantity of data points. A model with a smaller value of AICc is deemed likely more correct [25].

$$AICc=2p+n\ln\left(\frac{RSS}{n}\right)+2(p+1)+\frac{2(p+1)(p+2)}{n-p-2} \qquad \textbf{(Eqn. 4)}$$

## RESULTS AND DISCUSSIONS

Of the two models, the best performance was the Logistic model with the lowest value for RMSE, AICc and the highest value for adjusted $R^2$ (**Table 1**). The Logistic model was then utilized to model the growth data (**Fig. 1**). The result indicates maximal growth occurred after 15 h.p.i and the specific growth rate appears slightly higher for SARS-CoV than SARS-CoV-2 but this require analysing the confidence interval value. The coefficients for the model are shown in **Table 2**.

**Table 1**. Error function analysis between the two models utilized to model the growth curves of SARS-CoV and SARS-CoV-2 in Vero E6 cells.

| Model | SARS-CoV | | | SARS-CoV-2 | | |
|---|---|---|---|---|---|---|
| | $adjR^2$ | RMSE | AICc | $adjR^2$ | RMSE | AICc |
| Modified Gompertz | 0.9533 | 0.5227 | -33.05 | 0.8921 | 0.5709 | -27.41 |
| Modified Logistics | 0.9692 | 0.4247 | -46.34 | 0.9194 | 0.4934 | -36.74 |

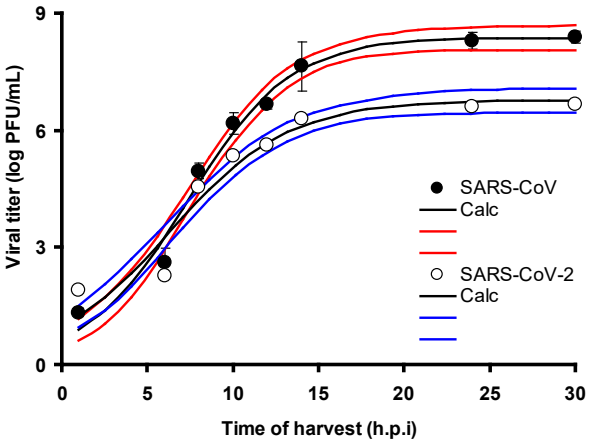


**Fig. 1**. Modelling of the growth curves of SARS-CoV and SARS-CoV-2 in Vero E6 cells. Solid black line indicates best fit curve whilst solid red and blue lines represent 95% confidence interval bands for SARS-CoV and SARS-CoV-2, respectively.

**Table 2**. Growth parameters based on the logistic model for the growth of SARS-CoV and SARS-CoV-2 in Vero E6 cells.

| Growth parameters | SARS-CoV | SARS-CoV-2 |
|---|---|---|
| $y_{max}$ | 8.067 to 8.690 | 6.428 to 7.135 |
| $A$ | 0.4100 to 0.9427 | 0.5613 to 1.421 |
| $\mu_m$ | 0.2856 to 0.3979 | 0.2269 to 0.3644 |

Note:
A= viral titer log (PFU/mL) lower asymptote;
$\mu_m$= maximum specific viral titer log (PFU/mL) growth rate;
λ=lag time (h.p.i)
$y_{max}$= Viral titer log (PFU/mL) upper asymptote;

The overlapping of the 95% confidence intervals for the parameters $A$ (lower asymptote value of viral titer) and $\mu_m$ (maximum specific viral titer) in the modified Logistics model (**Table 2**) which can also be visualized (**Fig. 1**) indicate no significant differences [26] between the parameters. However, the $y_{max}$ or viral titer log (PFU/mL) upper asymptote values did not overlap suggesting significant differences between the two values with viral titer values for SARS-CoV (SARS) value higher than SARS-CoV-2 (COVID-19). The biological significance of this finding needs further studies especially when a mathematical model of infection study in human infection has shown that the growth rate of SARS-CoV-2 (COVID-19) is double to that of SARS-CoV (SARS) [27]. Both of the logistic and the Gompertz curves have found utility in modelling the growth of HIV-1-positive population in Finland in population dynamics [28] and in *in vitro* growth of several viruses [29–31].

## CONCLUSION

In this work, the modelling of the growth of the viruses SARS-CoV-2 and SARS-CoV in Vero E6 cells is reported for the first time. Two commonly used models; modified Gompertz and modified Logistics were utilized and of the two, the best performance was the logistic model with the lowest value for RMSE, AICc and the highest value for adjusted $R^2$. The logistic models revealed overlapping of the 95% confidence intervals for the parameters $A$ (lower asymptote value of viral titer) and $\mu_m$ (maximum specific viral titer) indicating no significant differences between the parameters. However, the $y_{max}$ or viral titer log (PFU/mL) upper asymptote values did not overlap suggesting significant differences between the two values with viral titer values for SARS-CoV (SARS) value higher than SARS-CoV-2 (COVID-19). Further refinement to the experiment can be done by introducing bootstrapping and Monte Carlo simulation on the overlapped confidence interval values of the two parameters to assess significance.

## REFERENCES


1. Worldodometers. Coronavirus Update (Live): 10,590,724 Cases and 514,020 Deaths from COVID-19 Virus Pandemic - Worldometer [Internet]. 2020 [cited 2020 Jul 1]. Available from: https://www.worldometers.info/coronavirus/#countries
2. Gorbalenya AE, Baker SC, Baric RS, de Groot RJ, Drosten C, Gulyaeva AA, et al. The species Severe acute respiratory syndrome-related coronavirus : classifying 2019-nCoV and naming it SARS-CoV-2. Nat Microbiol. 2020 Apr;5(4):536–44.
3. Schwartz DA, Graham AL. Potential Maternal and Infant Outcomes from Coronavirus 2019-nCoV (SARS-CoV-2) Infecting Pregnant Women: Lessons from SARS, MERS, and Other Human Coronavirus Infections. Viruses. 2020 Feb;12(2):194.
4. Desforges M, Le Coupanec A, Dubeau P, Bourgouin A, Lajoie L, Dubé M, et al. Human Coronaviruses and Other Respiratory Viruses: Underestimated Opportunistic Pathogens of the Central Nervous System? Viruses. 2020 Jan;12(1):14.
5. Hageman JR. The Coronavirus Disease 2019 (COVID-19). Pediatr Ann. 2020 Mar 11;49(3):e99–100.
6. Segars J, Katler Q, McQueen DB, Kotlyar A, Glenn T, Knight Z, et al. Prior and novel coronaviruses, Coronavirus Disease 2019 (COVID-19), and human reproduction: what is known? Fertil Steril. 2020 Jun 1;113(6):1140–9.
7. Hirano T, Murakami M. COVID-19: A New Virus, but a Familiar Receptor and Cytokine Release Syndrome. Immunity. 2020 May 19;52(5):731–3.
8. Petrosillo N, Viceconte G, Ergonul O, Ippolito G, Petersen E. COVID-19, SARS and MERS: are they closely related? Clin Microbiol Infect. 2020 Jun 1;26(6):729–34.
9. South AM, Diz DI, Chappell MC. COVID-19, ACE2, and the cardiovascular consequences. Am J Physiol-Heart Circ Physiol. 2020 Mar 31;318(5):H1084–90.
10. Li G, He X, Zhang L, Ran Q, Wang J, Xiong A, et al. Assessing ACE2 expression patterns in lung tissues in the pathogenesis of COVID-19. J Autoimmun. 2020 Apr 13;102463.
11. Leung JM, Yang CX, Tam A, Shaipanich T, Hackett T-L, Singhera GK, et al. ACE-2 expression in the small airway epithelia of smokers and COPD patients: implications for COVID-19. Eur Respir J [Internet]. 2020 May 1 [cited 2020 Jun 26];55(5). Available from: https://erj.ersjournals.com/content/55/5/2000688
12. Ogando NS, Dalebout TJ, Zevenhoven-Dobbe JC, Limpens RWAL, van der Meer Y, Caly L, et al. SARS-coronavirus-2 replication in Vero E6 cells: replication kinetics, rapid adaptation and cytopathology. J Gen Virol [Internet]. 2020 [cited 2020 Jun 25]; Available from: https://www.microbiologyresearch.org/content/journal/jgv/10.1099/jgv.0.001453
13. Woolsey C, Borisevich V, Prasad AN, Agans KN, Deer DJ, Dobias NS, et al. Establishment of an African green monkey model for COVID-19. bioRxiv [Internet]. 2020 May 17 [cited 2020 Jun 26]; Available from: https://www.ncbi.nlm.nih.gov/pmc/articles/PMC7263506/
14. Takayama K. In Vitro and Animal Models for SARS-CoV-2 research. Trends Pharmacol Sci [Internet]. 2020 May 30 [cited 2020 Jun 26]; Available from: http://www.sciencedirect.com/science/article/pii/S0165614720301292
15. Zwietering MH, Jongenburger I, Rombouts FM, Van't Riet K. Modeling of the bacterial growth curve. Appl Environ Microbiol. 1990;56(6):1875–81.
16. Halmi MIE, Shukor MS, Johari WLW, Shukor MY. Modeling the growth curves of *Acinetobacter* sp. strain DRY12 grown on diesel. J Environ Bioremediation Toxicol. 2014;2(1):33–7.
17. Halmi MIE, Shukor MS, Masdor NA, Shamaan NA, Shukor MY. Evaluation of several mathematical models for fitting the growth of sludge microbes on PEG 600. J Environ Microbiol Toxicol. 2015;3(1):1–5.
18. Shukor MS, Shukor MY. Statistical diagnostic tests of residuals from the Gompertz model used in the fitting of the growth of *E. coli* measured using a real-time impedimetric biosensor. Nanobio Bionano. 2015;2(2):58–62.
19. Rohatgi A. WebPlotDigitizer. http://arohatgi.info/WebPlotDigitizer/app/ Accessed June 2 2014.; 2015.
20. Halmi MIE, Shukor MS, Johari WLW, Shukor MY. Mathematical modelling of the degradation kinetics of *Bacillus cereus* grown on phenol. J Environ Bioremediation Toxicol. 2014;2(1):1–5.
21. Khare KS, Phelan Jr FR. Quantitative comparison of atomistic simulations with experiment for a cross-linked epoxy: A specific volume–cooling rate analysis. Macromolecules. 2018;51(2):564–575.
22. Shukor MY. Bartlett and the Levene's tests of homoscedasticity of the modified Gompertz model used in fitting of *Burkholderia* sp. strain Neni-11 growth on acrylamide. Bioremediation Sci Technol Res. 2016 Jul 31;4(1):18–9.
23. Motulsky HJ, Ransnas LA. Fitting curves to data using nonlinear regression: a practical and nonmathematical review. FASEB J Off Publ Fed Am Soc Exp Biol. 1987;1(5):365–74.
24. Akaike H. New look at the statistical model identification. IEEE Trans Autom Control. 1974;AC-19(6):716–23.
25. Burnham KP, Anderson DR. Model Selection and Multimodel Inference: A Practical Information-Theoretic Approach. Springer Science & Business Media; 2002. 528 p.

26. Wijtzes T, Wit, Veld JHJ, Riet, t van, Zwietering M. Modelling bacterial growth of *Lactobacillus curvatus* as a function of acidity and temperature. Appl Environ Microbiol 61 1995 2533-2539. 1995 Jan 1;61.
27. Liang K. Mathematical model of infection kinetics and its analysis for COVID-19, SARS and MERS. Infect Genet Evol. 2020 Aug 1;82:104306.
28. Löytönen M. The Spatial Diffusion of Human Immunodeficiency Virus Type 1 in Finland, 1982-1997. Ann Assoc Am Geogr. 1991;81(1):127–51.
29. Tuitert G, Hofmeester Y. Epidemiology of beet necrotic yellow vein virus in sugar beet at different initial inoculum levels in the presence or absence of irrigation - Disease incidence, yield and quality. Eur J Plant Pathol. 1994;100(1):19–53.
30. Jiang J, Liang G, Zeng L. Influence of host age on the epizootic of nuclear polyhedrosis virus of *Spodoptera litura*. Chin J Appl Ecol. 2003;14(6):955–8.
31. Weiland CMa, Perez-Camacho F. Comparison of the logistic and gompertz equations to describe plant disease progress of grapevine fanleaf virus (GFLV) in “condado de huelva” (Spain) zone. Acta Hortic. 2004;652:305–8.